Reactions of Laser-Ablated Chromium Atoms with Nitric Oxide: Infrared Spectra of NCrO, Cr−(η^1-NO)$_X$ (x = 1, 2, 3, 4), and Cr-η^2-NO in Solid Argon

Mingfei Zhou and Lester Andrews*

Department of Chemistry, University of Virginia, Charlottesville, Virginia 22901

Received: April 7, 1998; In Final Form: July 1, 1998

Laser-ablated chromium atoms have been reacted with NO molecules during condensation in excess argon. Absorptions due to NCrO (976.1, 866.2 cm^{-1}), Cr−η^1-NO (1614.3, 541.1 cm^{-1}), and Cr−η^2-NO (1108.8, 528.2,478.0 cm^{-1}) are observed and identified via isotopic substitution and DFT frequency calculations. The insertion reaction to give the more stable NCrO product requires activation energy, while the addition products Cr−η^1-NO and Cr−η^2-NO can be formed on diffusion of cold reagents in solid argon. Higher nitrosyls are also formed on annealing. On the basis of isotopic multiplets, a 1623.3 cm^{-1} absorption is assigned to Cr−(η^1-NO)$_2$, a 1663.5 cm^{-1} absorption to Cr−(η^1-NO)$_3$, and absorptions at 1726.0, 663.0, and 506.1 cm^{-1} are assigned to Cr−(η^1-NO)$_4$. Evidence is also presented for the Cr−(η^1-NO)$_x^-$ anions (x = 1, 2, 3) absorbing 100−160 cm^{-1} lower than the neutral nitrosyl counterparts. In addition, NO complexes with CrO and CrO_2 are also observed.

Introduction

NO_x compounds are one of the most important pollutants from automobiles and aeronautics. There is an increasing study of the interaction of pollutant gas such as NO with metals in order to understand pollution reduction processes which involves catalytic removal on a metal surface.[1] Reactions of chromium atoms with NO are important in understanding reduction of NO on a catalytic chromium metal surface.[2] Ruschel et al. reported the matrix reactions of NO with thermal atoms of the second half of the first-row transition metals and identified metal nitrosyls.[3] Reactions of laser-ablated Al atoms and NO molecules have been investigated in this laboratory:[4] both addition products AlON and AlNO together with insertion product NAlO are trapped and identified via isotopic substitution and DFT calculations.

We are interested in understanding the mechanism of reactions of laser-ablated atoms, and reactions of laser-ablated metal atoms with oxygen and nitrogen molecules have been extensively studied in this laboratory.[5−12] Due to the availability of d orbitals, the chemistry of transition metals is quite different from the main group elements. Therefore, matrix isolation studies of laser-ablated transition metal atom reactions with NO have been carried out. In this paper, we report the first reaction of laser-ablated chromium atoms with NO. We will show that three CrNO isomers are produced, two addition and one insertion, and higher chromium nitrosyls are also trapped and identified from isotopic experiments. Only the stable chromium tetranitrosyl molecule has been studied previously.[13−15]

Experimental Section

The experimental apparatus and methods for laser ablation and FTIR matrix investigation have been described previously.[16] The 1064 nm Nd:YAG laser beam (Spectra Physics, DCR-11) was focused by an 10 cm focal length lens onto the rotating Cr metal target(Johnson Matthey, lump, 99.2%). The laser repetition rate is 10 Hz with pulse width of 10 ns. Laser energies ranging from 20 to 60 mJ/pulse were used in the experiments. The ablated metal atoms were co-deposited with 0.025−0.4% NO in argon onto the 10K CsI window at a rate of 2−4 mmol/h for 1−2 h. Several isotopic NO samples ($^{14}N^{16}O$, Matheson; $^{15}N^{16}O$, MDS Isotopes, 99%; $^{15}N^{18}O$, Isotec, 99%) and selected mixtures were used; reagent gases were condensed at 77 K, and the first vapor was removed to prepare the matrix sample. Infrared spectra were recorded with 0.5 cm^{-1} resolution and 0.1 cm^{-1} accuracy on a Nicolet 750 instrument. Matrix samples were annealed at different temperatures, and selected samples were subjected to broadband photolysis by a medium-pressure mercury arc lamp (Phillips, 175W) with the globe removed (240−580 nm).

Results

Infrared Spectra. The spectra of laser-ablated chromium atoms co-deposited with NO in excess argon (0.4% NO) are shown in Figures 1−3, and the product absorptions are listed in Table 1. In the 1900−1400 cm^{-1} nitrosyl stretching region, new absorption bands at 1726.0, 1696.8, 1663.5, 1623.3, 1614.3, 1609.1, 1548.9 1511.5, and 1463.1 cm^{-1} are observed after deposition. The stepwise annealing and photolysis behavior of these bands supports their identification from isotopic spectra, as will be discussed below. In the 1200−1100 cm^{-1} region, sharp bands were observed at 1108.8, 1132.2, and 1187.9 cm^{-1} after deposition.

In the 1000−800 cm^{-1} metal nitride and oxide stretching region, strong absorptions at 976.1, 970.1, and 866.2 cm^{-1} and weak absorptions at 986.5 and 873.0 cm^{-1} together with weak CrO absorption at 846.3 cm^{-1} and CrO_2 at 965.3 cm^{-1} were observed after deposition.

In addition, strong NO and $(NO)_2$ absorptions, weak N_2O (2218, 1282 cm^{-1}), NO_2 (1610.8 cm^{-1}), $(NO)_2^+$ (1589.4, 1583.4 cm^{-1}), $(NO)(NO)^-$ (1364.4 cm^{-1}), NO_2^- (1243.6 cm^{-1}), and three $(NO)_2^-$ isomers (1222.7, 1221.0, 1205.3 cm^{-1}) are observed after deposition.[17−20]

Several experiments were done using lower NO concentrations (0.1 and 0.025% NO) and lower laser power. Figure 4

S1089-5639(98)01780-0 CCC: $15.00
Published on Web 09/01/1998

TABLE 1: Infrared Absorptions (cm^{-1}) from Codeposition of Laser Ablated Chromium Atoms with NO in Excess Argon at 10 K

$^{14}N^{16}O$	$^{15}N^{16}O$	$^{15}N^{18}O$	$^{14}NO+^{15}NO$	$^{15}N^{16}O+^{15}N^{18}O$	*R*(14/15)	*R*(16/18)	assignment
1871.8	1830.9	1789.3	1871.8,1838.8	1839.0,1789.3	1.017 89	1.027 78	NO
1863.3	1830.5	1781.2	1863.3,1849.7	1830.5,1812.0	1.017 92	1.027 68	$(NO)_2$
1851.0	1816.7	1771.1	1830.5	1781.2	1.018 88	1.025 75	?
1797.9	1762.4	1721.0	1798.0,1762.4,1797.6	1762.4,1721.0,1763.5	1.020 14	1.024 06	ON-η^1-CrO
1776.2	1744.7	1697.5	1776.2,1757.6,1744.7	1744.7,1714.8,1697.5	1.018 05	1.027 81	$(NO)_2$
1726.0	1693.0	1652.2	1726.0,1715.7,1707.2,1699.8,1693.0	1693.0,1679.8,1669.3,1660.2,1652.2	1.019 49	1.024 69	Cr$-(\eta^1$-NO$)_4$
1696.8	1662.5	1626.1	1696.7,1662.6	1662.5,1626.1	1.020 63	1.022 38	Cr$-\eta^1$-η^2-$(NO)_2$
1668.7	1635.6	1595.8	1666.4,1653.8,1647.0,1634.5	1618.8,1609.5,1595.8	1.020 24	1.024 94	Cr$-(\eta^1$-NO$)_3$ site
1663.5	1631.6	1592.8			1.019 55	1.024 36	Cr$-(\eta^1$-NO$)_3$
1623.3	1590.7	1555.5	1623.3,1602.8, 1590.7	1590.7,1568.3,1555.5	1.020 49	1.022 63	Cr$-(\eta^1$-NO$)_2$
1614.3	1581.3	1546.4	1614.3,1581.3	1581.3,1546.4	1.020 87	1.022 57	Cr$-\eta^1$-NO site
1609.1	1576.6	1541.8	1609.1,1576.6	1576.6,1541.8	1.020 61	1.022 57	Cr$-\eta^1$-NO
1589.4	1562.0	1520.4			1.017 54	1.027 36	$(NO)_2^+$
1583.4	1556.3	1514.9			1.017 41	1.027 33	$(NO)_2^+$site
1577.4	1545.3	1512.0	1545.3		1.020 80	1.022 03	aggregate
1548.9	1517.6	1484.3	1549.0,1536.2,1526.2,1517.7	1517.6,1503.9,1493.5,1484.3	1.020 61	1.022 41	$Cr(NO)_3^-$
1511.5	1480.5	1449.7	1511.4,1480.6		1.020 97	1.021 25	$CrNO^-$
1497.5	1471.2	1431.8	1497.4,1471.2	1471.2,1431.8	1.017 86	1.027 53	aggregate
1463.1	1433.5	1402.8	1463.1,1445.0,1433.5	1433.5,1414.6,1402.8	1.020 76	1.021 25	$Cr(NO)_2^-$
1448.8	1423.0	1386.4	1448.4,1423.4	1422.4,1386.4	1.018 11	1.026 44	aggregate
1364.4	1341.5	1305.2			1.017 07	1.027 81	$(ON)(ON)^-$
1243.6	1218.3	1192.0	1243.6,1218.3	1218.3,1192.0	1.020 77	1.022 06	NO_2^-
1222.8	1198.8	1172.1	1222.8,1209.4,1198.8		1.020 02	1.022 78	cis-$(NO)_2-$
1221.0	1199.9	1167.4	1221.0,1209.4,1199.8	1199.9,1182.4,1167.4	1.017 58	1.027 84	trans-$(NO)_2^-$
1205.3	1181.5	1155.5			1.017 58	1.027 84	NNO_2^-
1187.9	1168.4	1139.1	1188.1,1168.4	1168.5,1139.1	1.016 69	1.025 72	η^2-NO-CrO_2
1165.2	1143.3				1.019 16		(Cr$-(\eta^2$-NO$)_2$)
1157.8	1136.8				1.018 47		(Cr$-(\eta^2$-NO$)_2$)
1132.2	1112.7	1088.0	1132.2,1127.5,1117.5,1112.6		1.017 52	1.022 70	Cr$-\eta^1$-η^2-$(NO)_2$
1108.8	1090.2	1062.6	1108.8,1090.5	1090.3,1062.6	1.017 06	1.025 97	Cr$-\eta^2$-NO
986.5	960.7	960.3	986.5,960.7		1.026 86	1.000 40	NCrO site
979.3	979.3	942.2				1.039 48	$(ON)_xCrO_2$
976.1	950.7	950.2	976.1,950.7		1.026 72	1.000 53	NCrO
970.1	970.1	933.7		970.1,956.0,933.7		1.038 98	η^2-NO-$^{52}CrO_2$
967.1	967.1	930.6		965.3,953.6,929.1		1.039 07	η^2-NO-$^{53}CrO_2$
965.3	965.3	929.1					$^{52}CrO_2$
962.3	964.3						$^{53}CrO_2$
892.2	888.8	857.2	891.8,889.1	888.7,857.2	1.003 83	1.036 86	(ON-$\eta^1)_3-$CrO
873.0	872.9	836.5		872.9,836.5	1.00 01	1.043 51	N^{52}CrO site
870.8	870.7	834.4			1.00 01	1.043 50	N^{53}CrO site
866.2	866.1	830.2		866.1,830.2	1.00 01	1.043 24	NCrO
864.7	864.6	828.7		864.5,828.7	1.00 01	1.043 32	N^{52}CrO site
862.6	862.4	826.6					N^{53}CrO site
847.0	847.0	808.3				1.047 88	?
846.3	846.3	809.6	846.3	846.3,809.6		1.045 33	CrO
663.0	655.7	648.5	663.0,661.2,659.5,657.6,656.2,654.4	655.1,653.5,652.5,651.8,649.7,648.5	1.011 13	1.011 10	Cr$-(\eta^1$-NO$)_4$
633.0	631.6	607.2	633.0,631.6	631.6,607.2	1.002 22	1.040 18	X-Cr_2O
541.1	537.3	524.3	541.1,537.3		1.007 07	1.024 79	Cr$-\eta^1$-NO site
533.3	529.6	517.0	533.4,529.6		1.006 99	1.024 37	Cr$-\eta^1$-NO
528.2	515.6	514.4			1.024 44	1.002 33	Cr$-\eta^2$-NO
506.1	495.1	487.4			1.022 21	1.015 80	Cr$-(\eta^1$-NO$)_4$
481.3	478.7	462.7	481.3,478.7		1.005 43	1.034 58	?
478.0	476.1	458.2	478.0,476.2		1.004 00	1.039 07	Cr$-\eta^2$-NO
460.9	457.2				1.008 09		?

shows spectra for lower laser power and a dilute (0.1% NO) sample, which favor the lower nitrosyl species. As will be discussed in the next section, the relative band intensities are changed, and different behaviors of product absorptions are observed.

Different isotopic nitric oxides $^{15}N^{16}O$, $^{15}N^{16}O+^{15}N^{18}O$ and $^{14}N^{16}O+^{15}N^{16}O$ mixtures were employed for product molecule identification through isotopic shifts and splittings of product bands. Selected spectra are shown in Figures 5 and 6, and the isotopic counterparts are listed in Table 1.

Calculations. Density functional theory calculations were performed on all the CrNO isomers using the Gaussian 94 program.[21] The BP86 functional[22,23] and 6-311+G* basis set[24,25] for N and O and Wachters−Hay set[26] for Cr as modified by Gaussian 94 were used for all calculations. Previous work has shown that the BP86 functional works well for metal systems particularly for frequency calculations.[6,11,12] The geometries and relative energies calculated for CrNO, CrON, NCrO, and cyclic Cr[NO] isomers in low lying states are listed in Table 2, and the isotopic frequencies, intensities, and isotopic frequency ratios for the ground-state structures are listed in Table 3. These calculations are considered as a first-order approximation to be used as a guide for vibrational assignments. For the NCrO molecule, the ground state is a bent $^2A''$ state, and the $^4A''$ state is 19.0 kcal/mol higher in energy. For CrNO, also known as Cr$-\eta^1$-NO, the calculated ground state is $^4\Sigma^-$, and the bent $^6A''$ state is 19.9 kcal/mol higher. Similar results have been reported by the Salahub group.[27] For cyclic Cr[NO], also known as Cr$-\eta^2$-NO, the ground state is $^4A''$, and the $^2A''$ state is 38.8 kcal/mol higher. For CrON, the $^4\Sigma^-$ state is lowest,

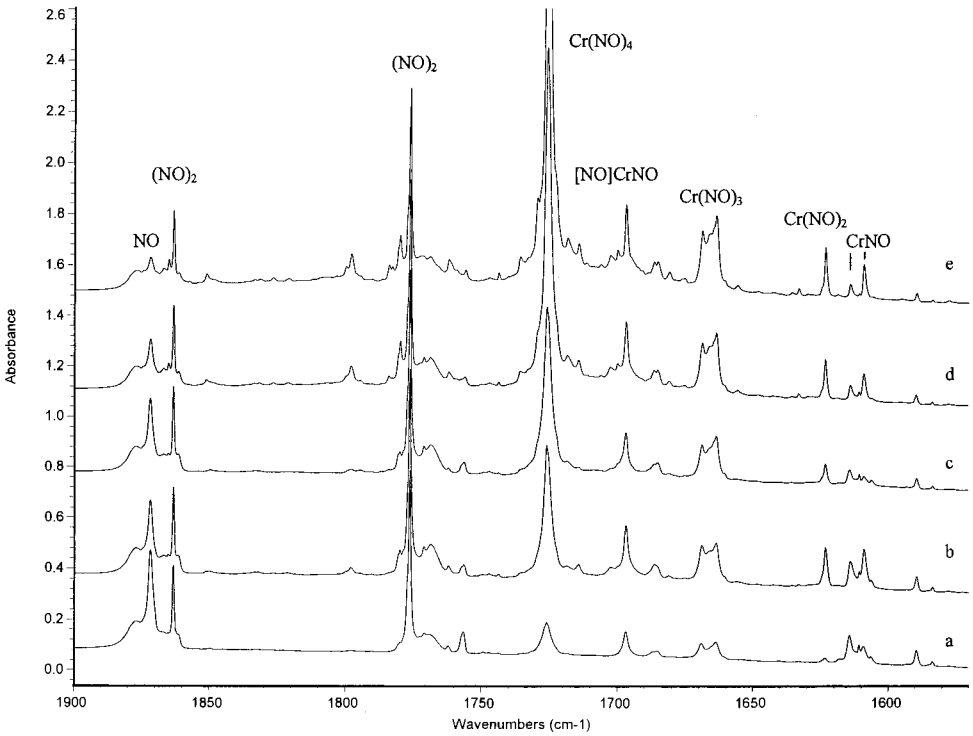

Figure 1. Infrared spectra in the 1900−1570 cm^{-1} region for laser-ablated chromium atoms co-deposited with 0.4% NO in excess argon on a 10 K CsI window: (a) after 1h sample co-deposition at 10 K, (b) after annealing to 25 K, (c) after broad-band photolysis for 30 min, (d) after annealing to 30 K, and (e) after annealing to 35 K. Labels in the figures employ NO or (NO) to denote η^1- and [NO] to denote η^2-bonding to Cr.

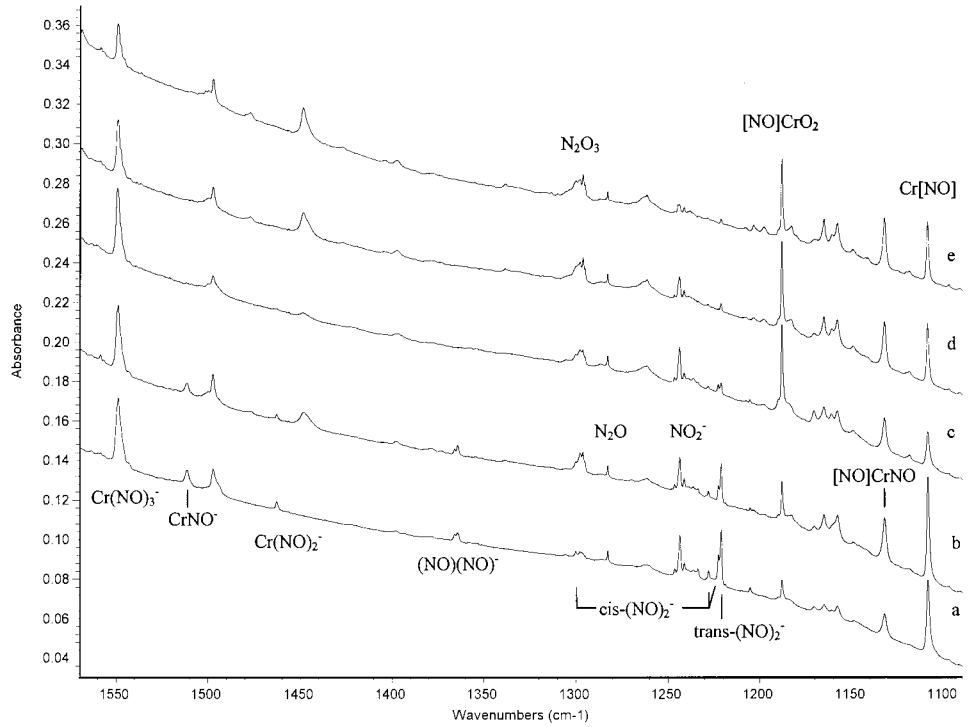

Figure 2. Infrared spectra in the 1570−1090 cm^{-1} region for spectra in Figure 1.

and the $^6A''$ state is 6.2 kcal/mol higher. Doublet NCrO is the global minimum at this level of theory, and the quartet CrNO, Cr[NO], and CrON states are 5.6, 16.4, and 39.4 kcal/mol higher in energy. The $^3\Sigma^-$ and $^5\Sigma^-$ anion $CrNO^-$ and the $^5\Pi$ cation $CrNO^+$ states were also calculated and are listed in Tables 2 and 3.

Similar calculations were also done for Cr−(η^1-NO)$_2$ and Cr−(η^1-NO)$_2^-$ anion, and the results are listed in Table 4.

Discussion

The new chromium-nitric oxide reaction products will be identified.

NCrO. In the previous Cr+O_2 experiments, the OCrO molecule was produced by insertion of Cr into dioxygen, while in the Cr+N_2 experiments, the NCrN molecule was formed by the reaction of N atoms with CrN molecules.[5,6] In those studies the resolution of natural Cr-52, -53, and -54 isotopic splittings

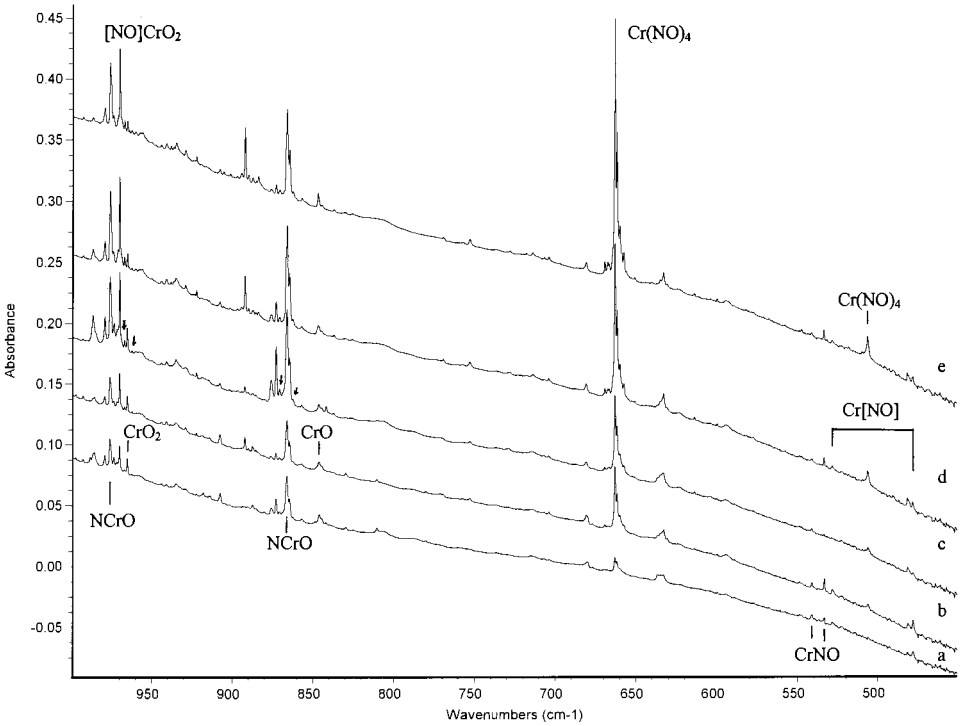

Figure 3. Infrared spectra in the 1000−450 cm^{-1} region for spectra in Figure 1. ^{53}Cr isotopic splittings are noted by arrows in scan (c).

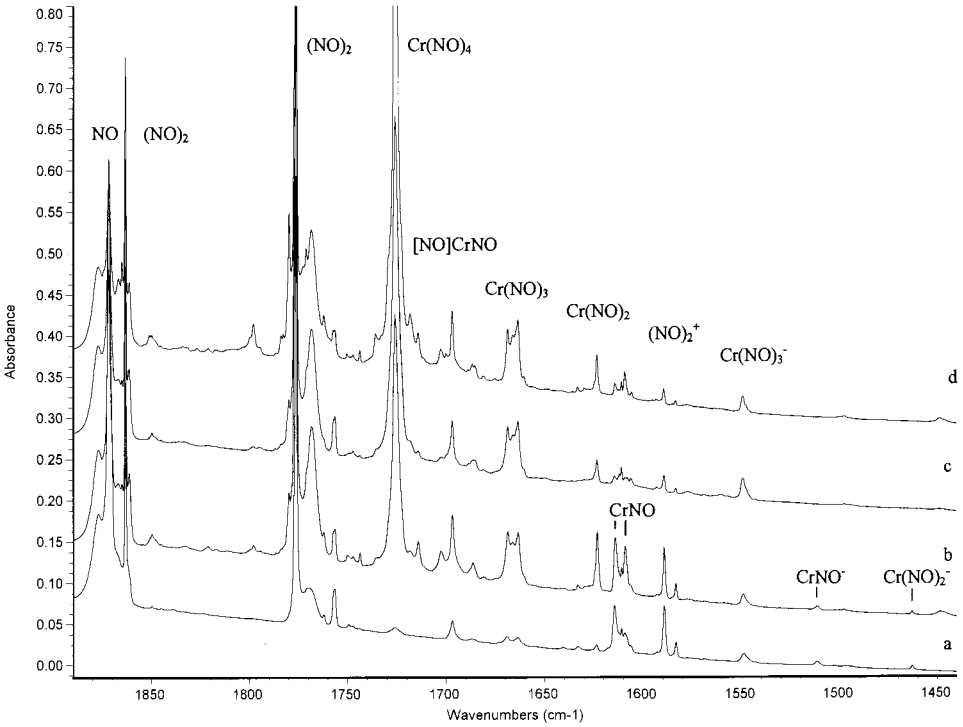

Figure 4. Infrared spectra in the 1900−1440 cm^{-1} region for laser ablated chromium atoms co-deposited with 0.1% NO in excess argon on a 10 K CsI window: (a) after 1 h deposition, (b) after annealing to 25 K, (c) after broad-band photolysis for 30 min, and (d) after annealing to 30 K.

for OCrO and NCrN indicated the presence of a single Cr atom and the same laser energy (and thus Cr atom concentration) was employed here. Accordingly, one of the interests in this study is to determine if the insertion reaction can occur for atomic Cr and NO. The 976.1 and 866.2 cm^{-1} bands observed after deposition, doubled on photolysis, and decreased slightly on annealing. The 976.1 cm^{-1} band shifts to 950.7 cm^{-1} with $^{15}N^{16}O$; the 14−16/15−16 ratio 1.02672 is very close to the diatomic CrN ratio (1.0273), while the oxygen isotopic shift is only 0.4 cm^{-1}. In contrast, the 866.2 cm^{-1} band shifts to 866.1 cm^{-1}, and the 15−16/15−18 isotopic ratio 1.04324 is slightly lower than the diatomic CrO ratio (1.0453). Only pure isotopic bands were observed in the mixed $^{14}N^{16}O+^{15}N^{16}O$ and $^{15}N^{16}O+^{15}N^{18}O$ experiments for both bands, indicating that only single O and N atoms are involved in the vibrations. Although the major $N^{52}CrO$ absorptions at 866.2 and 976.1 cm^{-1} are complicated by matrix site splittings, the natural abundance $N^{53}CrO$ counterparts of $N^{52}CrO$ site bands at 873.0 and 864.7

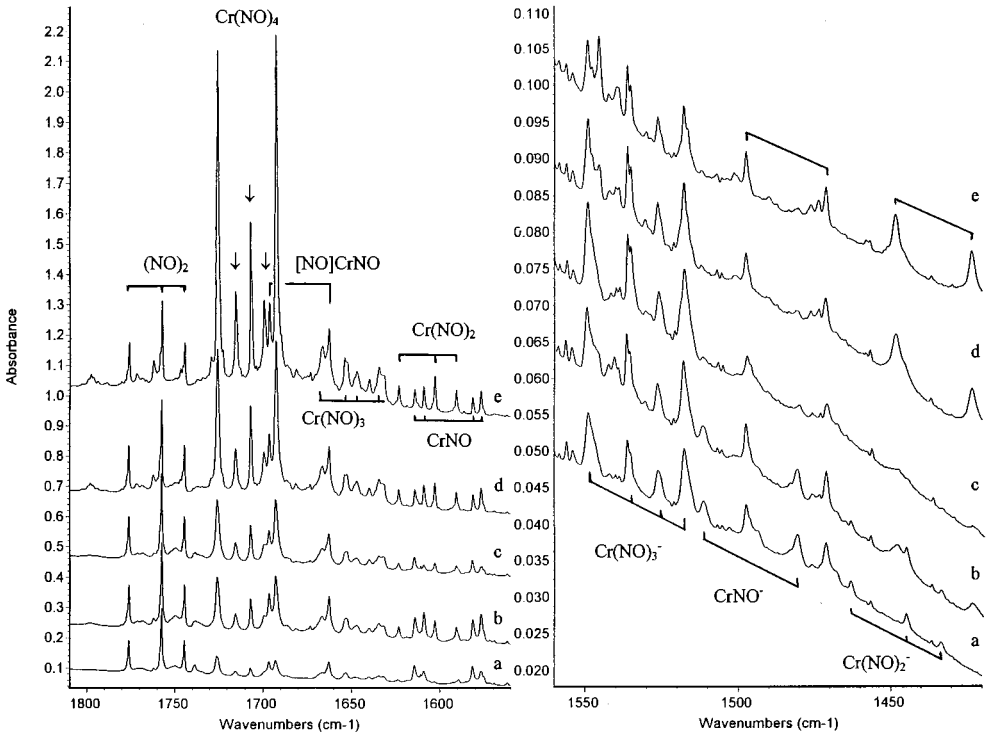

Figure 5. Infrared spectra in the 1810-1420 cm^{-1} region for laser-ablated chromium atoms co-deposited with 50% $^{14}N^{16}O$ + 50% $^{15}N^{16}O$ in excess argon at 10 K: (a) after 1 h deposition, (b) after 25 K annealing, (c) after 30 min broadband photolysis, and (d) after annealing to 35 K.

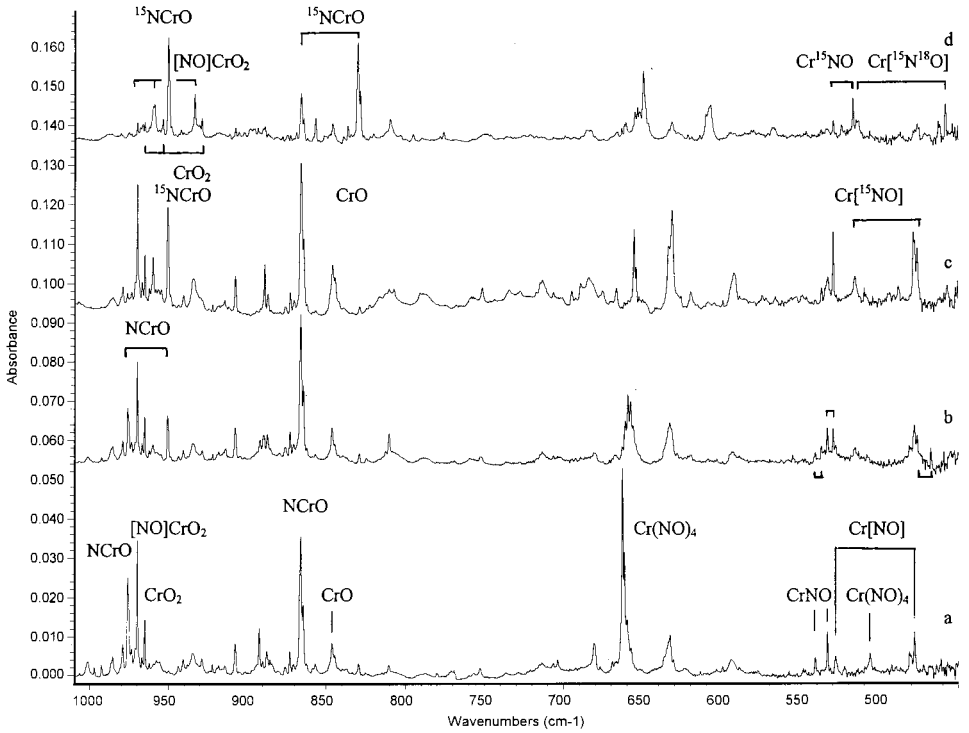

Figure 6. Infrared spectra in the 1010−450 cm^{-1} region for laser-ablated chromium atoms co-deposited with isotopic NO samples after annealing to 25 K: (a) pure $^{14}N^{16}O$, (b) 50%$^{14}N^{16}O$ + 50%$^{15}N^{16}O$, (c) pure $^{15}N^{16}O$, and (d) 30%$^{15}N^{16}O$ + 70%$^{15}N^{18}O$.

cm^{-1} were resolved at 870.8 and 862.6 cm^{-1} with one-eighth of the relative intensity. This provides spectroscopic evidence for a single Cr atom in the species absorbing at 866.2 and 976.1 cm^{-1}. Accordingly, a NCrO molecule is suggested.

DFT/BP86 calculations using 6-311+G* basis sets confirm this assignment and predict a $^2A''$ ground state for the bent NCrO molecule. The calculated frequencies for the CrN and CrO stretching modes are 1096.5 and 942.1 cm^{-1}, higher than the observed values by 12.3 and 8.8%, respectively, but the isotopic ratios calculated for each mode (14−16/15−16: 1.0271, 1.0001. 15−16/15−18: 1.0037, 1.0445.) are in excellent agreement with the experimental ratios (Table 1). We have found in general that NMO multiply bonded metal nitride−oxide insertion products are more difficult to model by calculation than the simple metal addition products;[28,29] this is due presumably to the presence of other low-lying configurations in the metal

TABLE 2: Relative Energies and Geometries Calculated (BP86/6-311+G*) for CrNO Isomer States

molecule	state	relative energies[a] (kcal/mol)	geometry (Å, deg)
NCrO	$^2A''$	0.0	CrN: 1.547. CrO: 1.624. ∠NCrO: 114.4°
CrNO[b]	$^4\Sigma^-$	+5.6	CrN: 1.667. NO: 1.212. ∠CrNO: 180°
Cr[NO][c]	$^4A''$	+16.4	CrN: 1.760. CrO: 1.859. NO: 1.343
NCrO	$^4A''$	+19.0	CrN: 1.625. CrO: 1.623. ∠NCrO: 111.6°
CrNO[a]	$^6A''$	+25.5	CrN: 1.894. NO: 1.206 ∠CrNO: 130.0°
CrON	$^4\Sigma^-$	+39.4	CrO: 1.772. ON: 1.252. ∠CrON: 180°
CrON	$^6A''$	+45.6	CrO: 2.020. ON: 1.209. ∠CrON: 125.0°
Cr[NO][c]	$^2A''$	+55.2	CrN: 1.662. CrO: 1.807. ON: 1.370
$CrNO^-$	$^5\Sigma^-$	−17.8	CrN: 1.725. NO: 1.247. ∠CrNO: 180°
$CrNO^-$	$^3\Sigma^-$	−20.7	CrN: 1.660. NO: 1.238. ∠CrNO: 180°
$NCrO^-$	$^1A'$	−24.1	CrN: 1.580. CrO: 1.673. ∠NCrO: 123.0°
$CrNO^+$	$^5\Pi$	+153	CrN: 1.804. NO: 1.158. ∠180°

[a] Without zero point energy correction. [b] Also known as Cr−η^1-NO and described as the end-bonded nitrosyl species. [c] Also known as Cr−η^2-NO and described as the side-bonded ring species.

TABLE 3: Isotopic Frequencies (cm^{-1}), Intensities (km/mol), and Ratios of Frequencies Calculated (BP86/6-311+G*) for the Ground-State Structures Described in Table 2

	14-16	15-16	15-18	*R*(14-16/15-16)	*R*(15-16/15-18)
NCrO	383.7(4)	378.1(4)	370.0(4)	1.0148	1.0219
($^2A''$)	942.1(179)	942.0(180)	901.9(162)	1.0001	1.0445
	1096.5(91)	1067.6(86)	1067.2(92)	1.0271	1.0004
CrNO	316.3(26)	308.3(24)	304.4(25)	1.0259	1.0128
($^4\Sigma^-$)	601.0(10)	596.7(9)	581.9(10)	1.0072	1.0254
	1653.9(487)	1619.3(471)	1584.0(444)	1.0214	1.0223
Cr[NO]	448.2(23)	445.9(23)	428.6(22)	1.0052	1.0404
($^4A''$)	570.9(15)	557.4(14)	555.5(14)	1.0242	1.0034
	1101.6(120)	1083.0(117)	1052.8(109)	1.0172	1.0287
$CrNO^-$	305.6(4)	297.8(4)	294.1(4)	1.0262	1.0126
($^3\Sigma^-$)	591.0(0.2)	587.0(0.1)	572.0(0.2)	1.0068	1.0262
	1535.9(785)	1503.1(757)	1471.6(719)	1.0218	1.0214
$CrNO^+$	235.3(18)	229.5(18)	226.4(17)	1.0253	1.0137
($^5\Pi$)	251.0(11)	244.8(11)	241.4(11)	1.0253	1.0141
	465.2(1)	460.9(1)	451.2(1)	1.0098	1.0215
	1862.1(301)	1826.8(287)	1780.4(276)	1.0193	1.0261

TABLE 4: Calculated (BP86/6-311+G*) Isotopic Frequencies (cm^{-1}) and Intensities (km/mol) for Cr−(η^1-NO)$_2$ and Cr−(η^1-NO)$_2^-$ Anion

	a_1	a_2	b_2	b_1	a_1	b_2	a_1	b_2	a_1
Cr−(η^1-NO)$_2$[a]	93.0	262.7	332.7	334.8	570.7	606.9	658.7	1656.8	1723.3
($^3B_2$)	(1)	(0)	(0.4)	(39)	(1)	(3)	(1)	(1283)	(309)
15-16, 15-16	92.8	256.1	324.4	326.6	559.2	602.2	647.5	1623.5	1688.4
	(1)	(0)	(0.3)	(37)	(1)	(4)	(1)	(1226)	(298)
15-18, 15-18	88.4	252.3	319.5	323.0	549.1	589.2	640.5	1585.7	1649.5
	(1)	(0)	(0.4)	(38)	(1)	(3)	(1)	(1179)	(282)
Cr−(η^1-NO)$_2^-$[b]	65.3	300.8	301.0	380.0	508.0	605.4	620.4	1483.8	1539.4
($^2A_1$)	(1)	(0)	(4)	(42)	(1)	(3)	(19)	(1359)	(478)
15-16, 15-16	65.1	293.2	293.7	370.6	496.2	601.1	612.6	1453.0	1506.8
	(1)	(0)	(4)	(39)	(1)	(2)	(17)	(1308)	(462)
15-18, 15-18	62.2	288.9	288.9	367.2	487.9	589.0	602.1	1421.2	1474.7
	(1)	(0)	(4)	(40)	(1)	(3)	(18)	(1243)	(435)

[a] Structure: Cr−N, 1.695 Å; N−O, 1.195 Å; ∠NCrN, 102.1°. [b] Structure: Cr−N, 1.696 Å; N−O, 1.239 Å; ∠NCrN, 122.0°.

multiple bond. Compared with the diatomic CrN frequency, the CrN stretching mode of NCrO is red shifted 68 cm^{-1}, while the CrO stretching mode is blue shifted 20 cm^{-1} with respect to diatomic CrO in solid argon.[5,6] Note that the BP86 calculation correctly predicts virtually no mode mixing. On the other hand, the $^4A''$ state that is 16.4 kcal/mol higher has lower frequencies, which are mixed bond stretching modes with markedly different isotopic ratios.

The bent NCrO molecule (calculated angle 114.4°) may be compared with the related NCrN and OCrO molecules, which have 109 ± 4° and 128 ± 4° angles deduced from isotopic frequencies and 956, 875 cm^{-1} and 965, 914 cm^{-1} stretching frequencies, respectively.[5,6] Note that the Cr−N stretching frequency for NCrO (976 cm^{-1}) is 61 cm^{-1} *higher* than the average for NCrN and the Cr−O mode for NCrO (866 cm^{-1}) is 79 cm^{-1} *lower* than the average stretching frequency for OCrO. Bond lengths calculated by DFT follow this trend. Clearly, chromium forms a stronger bond to nitrogen than to oxygen on a level playing field.

The 986.5 and 873.0 cm^{-1} bands decreased more than the 976.1 and 866.2 cm^{-1} bands on annealing and markedly increased on photolysis. The 873.0 cm^{-1} band exhibits the same isotopic ratio as the 866.2 cm^{-1} band, while the 986.5 cm^{-1} band is usually broad and has the same isotopic ratio as the 976.1 cm^{-1} band. These bands are assigned to the NCrO molecule in a different matrix environment.

The NCrO absorptions observed on deposition *decreased* on annealing, which indicates that NCrO must be produced by the insertion reaction 1 with energetic chromium atoms during the deposition process, and activation energy is required. Laser-ablated chromium atoms undergo reactions that require excess kinetic/electronic energy.[5,6] Note that broad-band photolysis

greatly increased the NCrO absorptions, so photolysis can also initiate the insertion reaction.

$$Cr^* + NO \rightarrow NCrO \quad (1)$$

CrNO also Cr−η^1-NO. Sharp 1614.3 and 1609.1 cm^{-1} bands were observed after deposition. These bands increased markedly upon first annealing to 25 K, further increased upon 30 and 35 K annealing, and slightly decreased on further annealing to 40 K. In the low NO concentration experiments, the relative yield of these bands increased compared with that of the 1623.3, 1726.0 cm^{-1} bands, which are due to higher nitrosyls. Two weak bands at 541.1 and 533.3 cm^{-1} behaved exactly the same as the 1614.3 and 1609.1 cm^{-1} bands, decreasing about 70% on photolysis and maintaining constant relative intensities with sample dilution over an order of magnitude concentration range. Furthermore, in the most dilute NO experiment (0.025%), only the two 1614.3 and 1609.1 cm^{-1} bands and the new 1623.3 cm^{-1} band were observed in the nitrosyl region, and Figure 4 spectra (0.1% NO) show 1614.3 cm^{-1} to be the strongest product band in this region.

The isotopic 14−16/15−16 ratios for the upper two bands are 1.020 87 and 1.020 61, slightly higher than the diatomic NO ratio (1.017 89), while the 15−16/15−18 ratio 1.022 57 is lower than the diatomic NO ratio (1.027 78), which means that the N atom is moving between O and another atom. In both the 14−16/15−16 and 15−16/15−18 mixed isotopic experiments, only pure isotopic counterparts for the four bands were observed. Therefore, the almost identical isotopic ratios and behavior in the experiments suggests that these bands are due to the same molecule at different matrix sites. The CrNO molecule must be considered.

The CrNO assignment is supported by DFT calculations. Blanchet et al.[27] calculated the N−O, and Cr−NO stretching frequencies for the $^4\Sigma^-$ ground state to be 1607 and 595 cm^{-1}. The N−O stretching mode is very close to our experimental observation, while the Cr−NO mode is slightly higher than the observed value. Our DFT/BP86 calculation predicts 1653.9 and 601.0 cm^{-1} for these two modes, which are 2.4 and 11.1% too high; however, the calculated isotopic ratios and intensities are in excellent agreement with the experimental values. Note that the N−O stretching mode is calculated more accurately than the Cr−N stretching mode. The calculated 14−16/15−16 and 15−16/15−18 isotopic ratios for the upper mode are 1.021 37 and 1.022 29, very close to the observed 1.020 87 and 1.022 57 ratios, while for the lower mode, calculations give 1.0072 and 1.025 43, and experiments provide 1.0070 and 1.024 37 ratios, respectively.

The CrNO absorptions markedly increased on first annealing, and slightly decreased upon 35−40 K annealing, indicating that this molecule can be formed on diffusion of cold reagents in solid argon:

$$Cr + NO \rightarrow CrNO \quad (2)$$

When available, NO can react further with CrNO to form higher nitrosyls:

$$CrNO + NO \rightarrow Cr(NO)_2 \quad (3)$$

$$Cr(NO)_2 + NO \rightarrow Cr(NO)_3 \quad (4)$$

$$Cr(NO)_3 + NO \rightarrow Cr(NO)_4 \quad (5)$$

The decrease of NO and increase of $(NO)_2$ absorptions on annealing attests to the diffusion and reaction of NO under these conditions.

$Cr(NO)_2$ also Cr−(η^1-NO)$_2$. The next band that increases on annealing in the nitrosyl region is at 1623.3 cm^{-1}. Similar to the CrNO bands, the 1623.3 cm^{-1} band decreases on photolysis, and the intensity relative to CrNO is higher in higher concentration NO experiments. This band shifts to 1590.7 cm^{-1} in the $^{15}N^{16}O$ experiment, and to 1555.5 cm^{-1} with $^{15}N^{18}O$, which exhibits 1.020 49 and 1.022 63 isotopic 14−16/15−16 and 15−16/15−18 ratios that are very similar to the ratios for CrNO. A 1:2:1 triplet is observed for both 14−16/15−16 and 15−16/15−18 isotopic mixtures, indicating that two equivalent NO submolecules are involved in this vibration. No other absorption is observed in the NO stretching region that tracks this band, and clearly the 1623.3 cm^{-1} band can be assigned to the $Cr(NO)_2$ molecule.

Similar DFT calculations predict a bent $^3B_2$ ONCrNO molecule (Table 4) with a very strong antisymmetric N−O stretching fundamental at 1656.8 cm^{-1}, just 3 cm^{-1} above CrNO, which is in good agreement with experiment. The calculated isotopic ratios, 1.02051 and 1.02384, are very close to the observed ratios. The symmetric N−O stretching mode is calculated to be much weaker and is not observed here.

$Cr(NO)_3$ also Cr−(η^1-NO)$_3$. The 1663.5 cm^{-1} band and 1668.7 cm^{-1} satellite observed on deposition doubles on first annealing to 25 K, increases slightly on subsequent annealing to 30, 35, and 40 K, while the 1726.0 cm^{-1} band due to $Cr(NO)_4$ greatly increased. In lower concentration NO experiments, similar behavior was observed, but the growth on annealing was less pronounced. The isotopic ratios (14−16/15−16: 1.019 55. 15−16/15−18: 1.024 36.) are characteristic nitrosyl ratios. In both 14−16/15−16 and 15−16/15−18 mixed experiments, quartets with approximate 2:1:1:2 relative intensities were observed, suggesting that three equivalent NO molecules are involved in a doubly degenerate stretching mode, and the $Cr(NO)_3$ molecule is proposed. This pattern is characteristic of the doubly degenerate stretching mode for a trigonal ligand complex with $F_r/F_{rr} = 10$ where r is the ligand stretching fundamental[30] (see Figure 2a in ref 30).

$Cr(NO)_4$ also Cr−(η^1-NO)$_4$. Chromium tetranitrosyl, $Cr(NO)_4$, is the only pure transition metal nitrosyl that has been characterized.[13−15] A strong NO stretching mode at 1725.5 cm^{-1} and a deformation band at 662.1 cm^{-1} have been observed in an argon matrix deposit containing the authentic material and at 1721 cm^{-1} in *n*-pentane and 650 and 496 cm^{-1} in Nujol.[14,15] In our experiments, the 1726.0 cm^{-1} band observed after deposition at higher NO concentrations greatly increased on annealing, and it became the strongest band in the experiments. Isotopic ratios again denote a nitrosyl vibration. Both mixed isotopic 14−16/15−16 and 15−16/15−18 experiments revealed a strong mixed isotopic pentet characteristic of a triply degenerate mode,[30] and the assignment to tetrahedral $Cr(NO)_4$ is confirmed. Two bands at 663.0 and 506.1 cm^{-1} track with the 1726.0 cm^{-1} band. The 663.0 cm^{-1} band has a very low 14/15 isotopic ratio (1.011 13), while the 506.1 cm^{-1} band has high 14/15 ratio (1.022 21). These two band are due to mixed triply degenerate Cr−N−O deformation and Cr−NO stretching modes of the $Cr(NO)_4$ molecule in agreement with the mull spectrum.

More information is available from the mixed isotopic pentet (see Figure 3 in ref 30). Compare the 3:1:2:1:3 relative intensities with the calculated spectrum in Figure 3a of ref 30; note the small asymmetry in the pentet to lower frequency, which points to the symmetric stretching mode at higher

frequency consistent with the Raman spectrum of the solid compound.[13]

Cr[NO] also Cr−η^2-NO. The 1108.8 cm^{-1} band observed after deposition, increased on annealing, but almost disappeared on photolysis. In $^{15}N^{16}O$ experiments this band shifts to 1090.2 cm^{-1}, and in $^{15}N^{18}O$ experiments to 1062.6 cm^{-1}. Both isotopic ratios, 1.017 06, 1.025 97, are slightly lower than the diatomic ratio, but still indicate an N−O stretching mode. A doublet is observed in the mixed 14−16/15−16 and 15−16/15−18 experiments, so another CrNO isomer must be considered. Our recent study on the Al+NO reaction system gave a strong absorption at 1282 cm^{-1} for AlON, based on isotopic ratios and DFT calculations.[4] Therefore, the CrON isomer first comes to mind; however, DFT calculations do not support assignment of this band to the CrON molecule as the ground state for the CrON molecule is calculated to be 39.4 kcal/mol higher than for NCrO. Furthermore, the calculated frequency for N−O stretching, 1440.3 cm^{-1}, is too high compared with the 1108.8 cm^{-1} observed band, and the calculated isotopic ratio *does not* match the observed values. Note that two very weak bands at 528.2 and 478.0 cm^{-1} band go together with the 1108.8 cm^{-1} band. The 528.2 cm^{-1} band exhibits a high 14/15 ratio (1.024 44) and a low 16/18 ratio (1.002 33), while the 478.0 cm^{-1} band has low 14/15 ratio (1.00400) and high 16/18 ratio (1.0397). Therefore, another CrNO isomer, cyclic or sideways bonded Cr[NO], must be considered.

As listed in Table 2, the calculated ground state for cyclic Cr[NO] is also a quartet, only 16.4 kcal/mol higher in energy than the most stable NCrO molecule. Note the calculated frequency 1101.6 cm^{-1} for the N−O stretching mode is very close to the observed 1108.8 cm^{-1} value. The calculated isotopic ratios for three modes of Cr[NO] are in excellent agreement with the experimental values, and these three bands are assigned to the cyclic Cr[NO] molecule. We note here that cyclic Sc[NO] and Ti[NO] are energetically more favorable than their ScON and TiON counterparts.[29]

The Cr[NO] absorptions observed after deposition increased on first annealing; therefore, this molecule can be formed via reaction 6 from cold reagents without activitation energy:

$$\mathrm{Cr+NO \rightarrow Cr[NO]} \qquad (6)$$

The absorptions of CrNO and Cr[NO] decreased on photolysis; one possibility is rearrangement to the more stable NCrO isomer molecule via photochemical rearrangement reactions 7 and 8:

$$\mathrm{CrNO} \xrightarrow{h\nu} \mathrm{NCrO} \qquad (7)$$

$$\mathrm{Cr[NO]} \xrightarrow{h\nu} \mathrm{NCrO} \qquad (8)$$

[NO]CrNO or Cr−(η^1-NO)−(η^2-NO). Two bands at 1132.2 and 1696.8 cm^{-1} appeared on deposition, increased together on annealing and decreased together on photolysis. The 1696.8 cm^{-1} band has higher 14−16/15−16 ratio and lower 15−16/15−18 ratio than the NO diatomic vibration, while for the 1132.2 cm^{-1} band the 14−16/15−16 and 15−16/15−18 ratios are both lower than the diatomic NO ratio, which is very similar to the ratio for the cyclic Cr[NO] molecule. An almost 1:1:1:1 quartet is observed in the 14−16/15−16 experiment for the 1132.2 cm^{-1} band, which indicates that this mode is coupled to an inequivalent N atom, while the 1696.8 cm^{-1} band reveals an apparent doublet, which shows no coupling to other N atoms. We assign these absorptions to the [ON]CrNO molecule with nitrosyl and side-bound NO submolecules.

The weaker 1165.2 and 1157.8 cm^{-1} bands also grow upon annealing and exhibit slightly higher 14−16/15−16 ratios, but 15−18 isotopic counterparts could not be observed. In the mixed 14−16/15−16 experiments, these bands gave triplet absorptions characteristic of two equivalent NO submolecules. These bands are tentatively assigned to the bicyclic Cr−(η^2-NO)$_2$ molecule.

The 1187.9 cm^{-1} band increases on annealing and markedly increases on photolysis, tracks with the 970.1 cm^{-1} band, and gives a doublet in mixed isotopic experiments. Because the 970.1 cm^{-1} band is most likely due to a CrO_2 subunit, these bands are tentatively assigned to [ON]CrO_2 or ON−η^2-CrO_2. Another band at 979.3 cm^{-1} has similar behavior, and is tentatively assigned to a higher nitrosyl of CrO_2.

Other absorptions. The weak band at 892.2 cm^{-1} produced upon annealing, destroyed upon photolysis, and increased markedly upon later annealing. With $^{15}N^{16}O$, this band shifts to 888.8 cm^{-1}, only 3.4 cm^{-1}. The $^{15}N^{18}O$ counterpart shifts to 857.2 cm^{-1}, and gives a 16/18 ratio 1.036 86, lower than the diatomic CrO ratio, but still characteristic of a terminal CrO vibration. The small ^{15}NO shift implies that this mode is slightly coupled to nitrogen. The NO stretching band at 1797.9 cm^{-1} tracks with the 892.2 cm^{-1} band. The mixed isotopic spectra are complicated: the broader 891.8, 889.1 cm^{-1} doublet observed with mixed $^{14}NO/^{15}NO$ is displaced inward from pure isotopic values and indicates the involvement of more than one NO subunit, and extra splittings are also observed on the 1797.9 cm^{-1} band. Annealing behavior in parallel to the 1726.0 cm^{-1} Cr(NO)$_4$ band suggests a saturated OCr−(η^1-NO)$_x$ species, and these bands are tentatively assigned to OCr−(η^1-NO)$_3$. DFT calculations performed on the ONCrO species predict a ^{2}A′ ground state with a strong CrO mode at 977 cm^{-1} with diatomic 16/18 ratio, and such a band is not observed here. A band at 866 cm^{-1} was assigned to OCCrO in the Cr+CO_2 system,[31] and a 856.9 cm^{-1} band was assigned to NNCrO molecule in the Cr+N_2O system.[5] Note that the 892.2 cm^{-1} CrO frequency is blue shifted 45.9 cm^{-1}, much more than the shift in NNCrO and OCCrO.

The weak 1851.0 cm^{-1} band increases on annealing and decreases on photolysis. The isotopic ratios indicate a nitrosyl vibration but this species cannot be identified. The 633.0 cm^{-1} band is in the region for dichromium oxide absorptions[5] and increase of this band with low NO and high Cr concentrations supports a dichromium species, which cannot be identified here. A number of bands that grow on annealing cannot be identified. Included are 1497.5 and 1448.0 cm^{-1} bands, which show nearly NO diatomic isotopic ratios. These are simply labeled "aggregates" in Table 1.

Charged Species. Both cations and anions have been observed in laser-ablated metal atom reaction experiments.[8,9,32,33] In these experiments, weak NO_2^- and $(NO)_2^+$ bands and three $(NO)_2^-$ isomers were observed after deposition.[17−20] Therefore, charged nitrosyl species can be produced and trapped in the matrix. In these experiments, weak bands observed at 1511.5 and 1463.1 cm^{-1} after deposition, decreased about 50% upon 25 K annealing, disappeared on photolysis, and did not reappear on further annealing. The relative yields of these bands increased in lower laser energy experiments. The same behavior was found for a cis and trans-$(NO)_2^-$ species also observed in these experiments.[20] Accordingly, charged Cr product species must also be considered.

DFT/BP86 calculations for the ground states of $CrNO^+$, CrNO, and $CrNO^-$ predict a 208 cm^{-1} *blue* shift for the cation and a 118 cm^{-1} *red* shift for the anion relative to the CrNO

nitrosyl stretching frequency. Similar predictions have been made[34] for $FeCO^+$, FeCO, and $FeCO^-$. Accordingly, the 1511.5 cm^{-1} absorption is in the region expected for $CrNO^-$. Unfortunately, no absorption was observed in the 1800 cm^{-1} region for $CrNO^+$. In the mixed experiments, the 1511.5 cm^{-1} band shows a doublet with $^{15}N^{16}O$ counterpart at 1480.5 cm^{-1} and $^{15}N^{18}O$ counterpart at 1449.7 cm^{-1}, which give the 14−16/15−16 ratio 1.020 97 and the 15−16/15−18 ratio 1.021 25. DFT calculations predict the N−O stretching frequency of the $CrNO^-$ ground state at 1509.2 cm^{-1} with 14−16/15−16 ratio of 1.021 25 and 15−16/15−18 ratio of 1.022 56, which are in good agreement with the observed ratios. Accordingly, this photosensitive absorption is assigned to $CrNO^-$. The $^3\Sigma$ state of $CrNO^-$ is 26.3 kcal/mol below the $^4\Sigma^-$ state of CrNO, and this energy difference is reasonable for the electron affinity of CrNO. We note that this calculated electron affinity for CrNO is higher than electron affinities for NO (0.6 kcal/mol) and Cr (15.6 kcal/mol).[35,36] Following the example of FeCO,[37] it is reasonable to expect the electron affinity of CrNO to exceed that of atomic Cr.

The 1463.1 cm^{-1} band is destroyed by photolysis like the 1511.1 cm^{-1} band, and a 1:2:1 triplet is observed in both 14−16/15−16 and 15−16/15−18 mixtures, which exhibits similar isotopic ratios with $CrNO^-$. The 1463.1 cm^{-1} band is appropriate for assignment to $Cr(NO)_2^-$. Similar DFT calculations predict a bent doublet $Cr(NO)_2^-$ anion with strong antisymmetric N−O stretching frequency at 1483.8 cm^{-1} and isotopic ratios in excellent agreement with the observed ratios. The energy of this doublet anion is 45.3 kcal/mol below the triplet $Cr(NO)_2$ species, which is an approximate calculation for the electron affinity of $Cr(NO)_2$. This prediction of electron affinity must be viewed with caution, as the electron affinity measured for $Fe(CO)_2$, i.e., 28.0 kcal/mol,[37] and the electron affinity for $Cr(CO)_3$, i.e., 31.3 kcal/mol,[36] are somewhat smaller.

The 1548.9 cm^{-1} band is slightly increased by broadband photolysis, which destroys the bands assigned to $CrNO^-$ and $Cr(NO)_2^-$. This band shows a 2:1:1:2 quartet with isotopic mixtures, such as $Cr(NO)_3$, and is in the position expected for the $Cr(NO)_3$- anion, which should have a higher detachment energy than $Cr(NO)_2$- and $CrNO^-$, based on the $Fe(CO)_x^-$ anions.[37] The photodetachment of $CrNO^-$ and $Cr(NO)_2^-$ with growth of $Cr(NO)_3^-$ requires this relationship. Accordingly, the 1548.9 cm^{-1} absorption is assigned to $Cr(NO)_3^-$. Note the absence of another band in this progression for a higher nitrosyl anion since $Cr(NO)_4$ is a closed shell species.

These anions are formed by electron capture during condensation from electrons produced in the laser ablation process.

$$Cr(NO)_x + e^- \rightarrow Cr(NO)_x^- \qquad (x = 1, 2, 3) \qquad (9)$$

$$(NO)_2 + e^- \rightarrow \textit{cis}\text{-}(NO)_2^- \quad \text{and} \quad \textit{trans}\text{-}(NO)_2^- \qquad (10)$$

Conclusions

Laser-ablated chromium atoms have been reacted with NO molecules during condensation in excess argon. Absorptions due to NCrO (976.1, 866.2 cm^{-1}), Cr−η^1-NO (1614.3, 541.1 cm^{-1}) and Cr−η^2-NO (1108.8, 528.2,478.0 cm^{-1}) are observed and identified via isotopic substitution and DFT frequency calculations. The insertion reaction to give the more stable NCrO product requires activation energy provided by the laser ablated Cr atoms, while the addition products Cr−η^1-NO and Cr−η^2-NO can be formed upon diffusion of cold reagents in solid argon. Higher nitrosyls are also formed upon annealing. On the basis of mixed isotopic multiplets, a 1623.3 cm^{-1} absorption is assigned to Cr−(η^1-$NO)_2$, a 1663.5 cm^{-1} absorption to Cr−(η^1-$NO)_3$, and absorptions at 1726.0, 633.0, and 506.1 cm^{-1} are assigned to Cr−(η^1-$NO)_4$. The observation of the known chromium tetranitrosyl molecule supports the reaction mechanism of the stepwise addition of four nitrosyl ligands to chromium.

Finally, evidence is presented for the anions $Cr(NO)_x^-$ (x = 1,2,3) produced by the capture of ablated electrons during the condensation process. These chromium nitrosyl anions have nitrosyl stretching vibrations 100−160 cm^{-1} *lower* than their neutral nitrosyl counterparts. In addition, the *cis*-$(NO)_2^-$ and *trans*-$(NO)_2^-$ anions[20] are observed in these experiments.

Acknowledgment. We gratefully acknowledge N.S.F. support under Grant CHE 97-00116.

References and Notes

(1) Ward, T. R.; Alemany, P.; Hoffmann, R. *J. Phys. Chem*. **1993**, *97*, 7691.
(2) Duffy, B. L.; Curry-Hyde, H. E.; Cant, N. W. *J. Catal.* **1994**, *149*, 11.
(3) Ruschel, G. K.; Nemetz, T. M.; Ball, D. W. *J. Mol. Struc*. **1996**, *384*, 101.
(4) Andrews , L.; Zhou, M. F.; Bare, W. D. *J. Phys. Chem. A*. **1998**, *102*, 5019.
(5) Chertihin, G. V.; Bare, W. D.; Andrews, L. *J. Chem. Phys.* **1997**, *107*, 2798.
(6) Andrews, L.; Bare W. D.; Chertihin, G. V. *J. Phys. Chem. A* **1997**, *101*, 8417.
(7) Andrews, L.; Chertihin, G. V.; Ricca, R.; Bauschlicher, C. W., Jr. *J. Am. Chem. Soc*. **1996**, *118*, 467.
(8) Andrews, L.; Burkholder, T. R.; Yustein, J. T. *J. Phys. Chem*. **1992**, *96*, 10182.
(9) Chertihin, G. V.; Andrews, L. *J. Phys. Chem*. **1995**, *99*, 6356.
(10) Chertihin, G. V.; Bare, W. D.; Andrews, L. *J. Phys. Chem. A* **1997**, *101*, 5090.
(11) Chertihin, G. V.; Andrews, L.; Rosi, M.; Bauschlicher, C. W., Jr. *J. Phys. Chem. A* **1997**, *101*, 9085.
(12) Chertihin, G. V.; Andrews, L.; Bauschlicher, C. W., Jr. *J. Am. Chem. Soc*. **1998**, *120*, 3205.
(13) Herberhold, M.; Razasi, A. *Angew. Chem., Int. Ed*. **1972**, *11*, 1092.
(14) Swanson, B. I.; Satija, S. K. *J. Chem. Soc., Chem. Commun*. **1973**, 40.
(15) Satija, S. K.; Swanson, B. I.; Crichton, O.; Rest, A. J. *Inorg. Chem*. **1978**, *17*, 1737.
(16) Hassanzadeh, P.; Andrews, L. *J. Phys. Chem*. **1992**, *96*, 9177.
(17) Milligan, D. E.; Jacox, M. E. *J. Chem. Phys*. **1971**, *55*, 3404.
(18) Hacaloglu, J.; Suzer, S.; Andrews, L. *J. Phys. Chem*. **1990**, *94*, 1759.
(19) Strobel, A.; Knoblauch, N.; Agreiter, J.; Smith, A. M.; Nerder-Schatteburg, G.; Bondybey, V. E. *J. Phys. Chem*. **1995**, *99*, 872.
(20) Andrews, L.; Zhou, M. F.; Willson, S. P.; Kushto, G. P.; Snis, A.; Panas, I. *J. Chem. Phys*. **1998**, *109*, 177.
(21) Frisch, M. J.; Trucks, G. W.; Schlegel, H. B.; Gill, P. M. W.; Johnson, B. G.; Robb, M. A.; Cheeseman, J. R.; Keith, T.; Petersson, G. A.; Montgomery, J. A.; Raghavachari, K.; Al-Laham, M. A.; Zakrzewski, V. G.; Ortiz, J. V.; Foresman, J. B.; Cioslowski, J.; Stefanov, B. B.; Nanayakkara, A.; Challacombe, M.; Peng, C. Y.; Ayala, P. Y.; Chen, W.; Wong, M. W.; Andres, J. L.; Replogle, E. S.; Gomperts, R.; Martin, R. L.; Fox, D. J.; Binkley, J. S.; Defrees, D. J.; Baker, J.; Stewart, J. P.; Head-Gordon, M.; Gonzalez, C.; Pople J. A. Gaussian 94, *Revision B.1*; Gaussian, Inc.: Pittsburgh, PA, 1995.
(22) Perdew, J. P. *Phys. Rev. B* **1986**, *33*, 8822.
(23) Becke, A. D. *J. Chem. Phys*. **1993**, *98*, 5648.
(24) McLean, A. D.; Chandler, G. S. *J. Chem. Phys*. **1980**, *72*, 5639.
(25) Krishnan, R.; Binkley, J. S.; Seeger, R.; Pople, J. A. *J. Chem. Phys*. **1980**, *72*, 650.
(26) Wachters, A. J. H. *J. Chem. Phys.* **1970**, *52*, 1033; Hay, P. J. *J. Chem. Phys.* **1977**, *66*, 4377.
(27) Blanchet, C.; Duarte, H. A.; Salahub, D. R. *J. Chem. Phys.* **1997**, *106*, 8778.
(28) Andrews, L.; Chertihin, G. V.; Citra, A.; Neurock, M. *J. Phys. Chem.* **1996**, *100*, 11235.
(29) Kushto, G. P.; Zhou, M. F.; Andrews, L.; Bauschlicher, C. W., Jr. To be published.
(30) Darling, J. H.; Ogden, J. S. *J. Chem. Soc., Dalton Trans*. **1972**, 2496.

(31) Souter, P. F.; Andrews, L. *J. Am. Chem. Soc.* **1997**, *119*, 7350.
(32) Chertihin, G. V.; Saffell, W.; Yustein, J. T.; Andrews, L.; Neurock, M.; Ricca, A.; Bauschlicher, C. W., Jr. *J. Phys. Chem.* **1996**, *100*, 5261.
(33) Chertihin, G. V.; Andrews, L. *J. Chem. Phys.* **1998**, *108*, 6404.
(34) Castro, M.; Salahub, D. R.; Fournier, R. *J. Chem. Phys.* **1994**, *100*, 8233.
(35) Travers, M. J.; Cowles, D. C.; Ellison, G. B. *Chem. Phys. Lett.* **1989**, *164*, 449.
(36) Bengali, A. A.; Casey, S. M.; Cheng, C.-L.; Dick, J. P.; Fenn, P. T.; Villalta, P. W.; Leopold, D. G. *J. Am. Chem. Soc.* **1992**, *114*, 5257.
(37) Engelking, P. C.; Lineberger, W. C. *J. Am. Chem. Soc.* **1979**, *101*, 5569.